

Analysis of Symmetry Breaking Bifurcation in Duffing System with Random Parameter

Ying Zhang¹, Lin Du¹, Xiaole Yue¹, Qun Han¹ and Tong Fang²

Abstract: The symmetry breaking bifurcation (SBB) phenomenon in a deterministic parameter Duffing system (DP-DS) is well known, yet the problem how would SBB phenomenon happen in a Duffing system with random parameter (RP-DS) is still open. For comparison study, the results for DP-DS are summarized at first: in short, SBB in DP-DS is just a transition of response phase trajectories from a single self-symmetric one about the origin into two mutual symmetric once, or vice versa. However, in DP-DS case, the two mutual symmetric phase trajectories are never commutable. In view of every sample of RP-DS is a DP-DS, we think that SBB phenomenon might also happen in a RP-DS as an ensemble mean behavior. Since the orthogonal polynomial approach is a practical method to study the dynamical behavior of nonlinear system with random parameters, so we apply the Chebyshev polynomials approach to reduce the RP-DS to an equivalent deterministic system (EDS) to study its dynamical behavior in ensemble average mean. Numerical simulations on both DP-DS and EDS show that though SBB may happen in similar apparent forms, but for EDS the two coexisting symmetric phase trajectories are occasionally commutable. We cannot but resort to study the different features of attractive basins for these two kind of mutual symmetric phase trajectories. We found that the boundary of attractive basins in EDS case is fractal-like, while that in DP-DS case is smooth.

Keywords: Duffing system, Symmetry breaking bifurcation, Random parameter, Chebyshev orthogonal polynomial approximation, attractive basin, basin boundary.

1 Introduction

Symmetry is ubiquitous in nature, and it appears in many classical nonlinear dynamical systems, such as Duffing system, van der Pol system and so on [Thompson

¹ School of Science, Northwestern Polytechnical University, Xian, China.

² School of Mechanics, Civil Engineering and Architecture, Northwestern Polytechnical University, Xian, China.

and Stewart (1986); Yue, Xu and Zhang (2012); Zhang and Guo (2013); Xu et al. (2013); Dai et al. (2014)]. One typical symmetric phenomenon in nonlinear dynamics is SBB, which has been studied for decades [Fang and Dowell (1987); Sunner and Sauermann (1993); Chen et al. (2001); Bishop et al. (2005); Zhang et al. (2009)]. It is easy to find that the self-symmetry has been broken after SBB, but in our previous research [Fang and Zhang (2008)] SBB operates just as a transition between different symmetry forms, while still preserving system's symmetry. In order to gain a further insight into the mechanism of SBB, a significant phase portrait for two newly born symmetric periodic motions is shown by the flow pattern of Poincaré mapping points, which reveals that SBB is always associated with a periodic saddle-node bifurcation. Based on the researches in deterministic system, we are still interested in the stochastic behaviors in Duffing system.

The stochastic phenomena of a nonlinear dynamical system have many incentives, such as exterior and interior stochastic excitation [Xu, Gu et al. (2011); Xu, Feng et al (2013, 2015)], stochastic initial condition (IC) [Mei (1992)], and system parameter uncertainty. What's more, the dynamical behaviors of stochastic fractional dynamical systems have also been studied in recent years [Xu, Li and Liu (2013, 2014)]. In this paper, we focus on the effect of parameter uncertainty, which is a common phenomenon in real world system [Zhang, Xu and Fang (2007); Xu et al. (2011); Ma et al. (2013)], and should not be ignored. For instance, the system parameters are usually random, ascribed to so many unavoidable uncertain factors in material, processes of measuring, manufacturing and installing. It is important to understand how the randomness of parameter influences the system, especially when it involves nonlinear dynamical behavior. To the best knowledge of us, this is an understudied problem in the literature, and very few works [Wang et al. (2013)] has explicitly focused on it from a global perspective. Therefore, an insight into the stability and dynamical behaviors of RP-DS is performed accordingly in this paper.

In order to research the stochastic structure dynamical system, three available fundamental mathematical methods are proposed. Stochastic perturbation method, which is restricted to the small fluctuation of random variables, gets higher calculating precision. Monte Carlo simulation method, which is one of the most commonly used and powerful approach, but it is computationally very intensive. Thus, the orthogonal polynomial approximation method is applied in this uncertainty problem because of its extensive applicability and reduced computation complexity, which is introduced by Spanos and Jensen [Spanos and Ghanem (1989); Jensen and Iwan (1992)].

Main works of this paper consist of three parts as follows. In Sect.2, symmetrical phenomena in DP-DS are finely investigated by analyzing phase trajectories, bifurcation diagram, top Lyapunov exponents and basins of attraction. In Sect.3,

Chebyshev orthogonal polynomial approach is used to reduce RP-DS to an EDS. Furthermore, the SBB in EDS are analyzed in Sect.4. Finally, the results and conclusions are drawn in Sect. 5.

2 Deterministic symmetry-breaking bifurcation in DP-DS

We present a Duffing oscillator subjected to a simple harmonic excitation as:

$$\ddot{x} + c\dot{x} + (1 + ax^2)x = F \cos \omega t, \quad (1)$$

where $F \cos \omega t$ is a given harmonic excitation, $a = 1.0$, $c = 0.2$, $F^2 = 40$ and ω are all constants. Let $x = x$, $\dot{x} = y$, Eq. 1 can be rewritten as:

$$\begin{aligned} \dot{x} &= y \\ \dot{y} &= -(1 + ax^2)x - cy + F \cos \omega t. \end{aligned} \quad (2)$$

The symmetry property of Eq. 2 has been analyzed in our previous work [Fang and Zhang (2008)]. Taking ω as a bifurcation parameter, the multi-bifurcation diagrams and the corresponding Top Lyapunov Exponent (TLE) diagrams are shown in Fig.1. From Fig. 1, 2 and Fig. 3, one can obviously see that with the increasing of ω , SBB and its inverse bifurcation occur at four different values of ω , and the forms of symmetry are changed accordingly when ω passes a certain critical value. Moreover, the TLEs become zero at each SBB point [Parker and Chua (1989); Ott (2002)].

An insight into the phenomena of post SBB in Poincaré section was given in our previous work [Fang and Zhang (2008)]. In Fig. 4(a), the flow lines are composed by discrete Poincaré mapping points of system (2); and in Fig. 4(b), we just keep the fined saddle point S, together with its invariant unstable manifolds SA, SB and parts of its stable manifolds CS, DS; while A and B are two stable nodes. Comparing with Fig. 4(c), it is clearly that stable manifolds of S are just lying on the basin boundary, and which is smooth. Since A and B are two isolated singular points and the flow lines of Poincare mapping points terminal at A or B are separated by this invariant unstable manifold of S, so that the phase trajectories corresponding to A or B never be commutable.

3 Orthogonal polynomial approach for RP-DS

Duffing system with random parameter c can be described as:

$$\ddot{x} + (\bar{c} + \sigma \xi)\dot{x} + (1 + ax^2)x = F \cos \omega t, \quad (3)$$

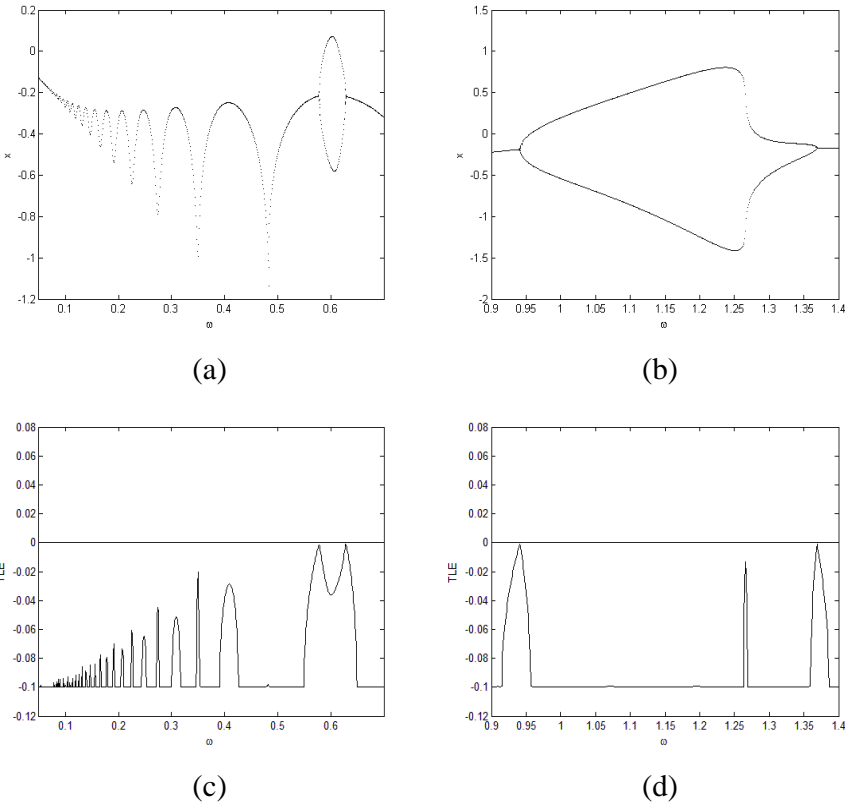


Figure 1: The multi-bifurcation diagrams of Eq.2, which are calculated from 60 different ICs. The parameter interval of (a) is $\omega \in (0.05, 0.7)$ and (b) is $\omega \in (0.9, 1.4)$; (c) and (d) are separated TLE diagrams.

where c is expressed as $c = \bar{c} + \sigma\xi$. Herein, \bar{c} is the mean value of c , ξ is a random variable under the arch-like distribution on $[-1, 1]$ and σ is the intensity of ξ [Fang, Leng and Song (2003)]. Such that, the response of system (3) is the function of t and ξ , and can be expressed as:

$$x(t, \xi) = \sum_{i=0}^N x_i(t)H_i(\xi). \tag{4}$$

Based on the relationships between the distributions and polynomials in Askey scheme, the associated second kinds of Chebyshev orthogonal polynomials are applied in series (4) as $\{H_i(\xi), i = 1, 2, \dots, n\}$, where N represents the largest order of polynomials we have taken. Only if $N \rightarrow \infty$, $\sum_{i=0}^N x_i(t)H_i(\xi)$ is strictly equal to

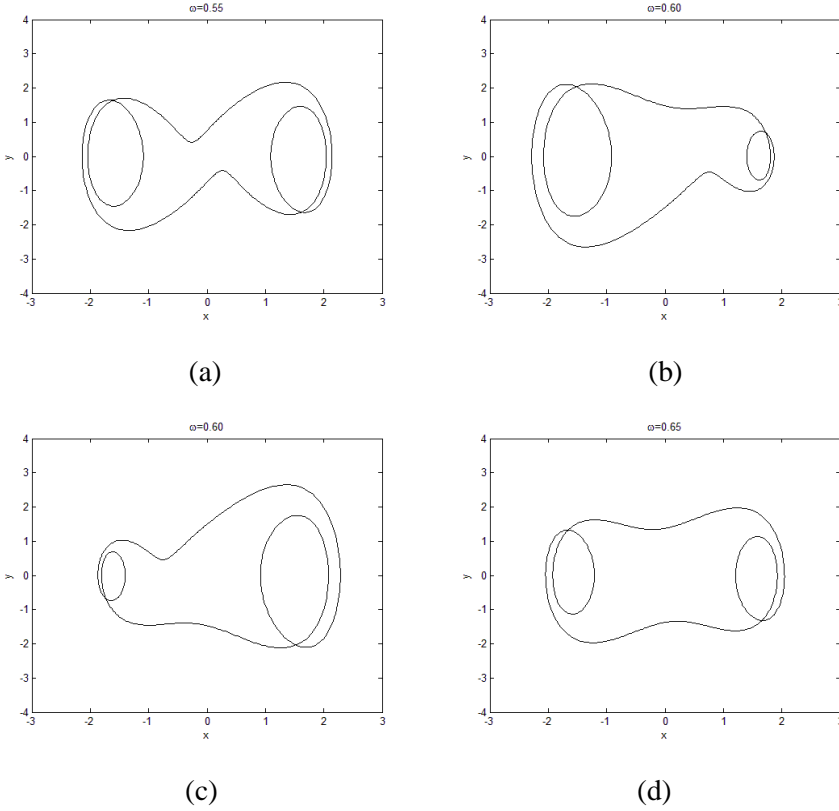


Figure 2: The periodic phase trajectories of Eq.2 with (a) $\omega = 0.55$ before SBB; when $\omega = 0.6$, (b) and (c) are two different ICs, after SBB; and (d) $\omega = 0.65$, after inverse SBB.

$x(t, \xi)$. In this paper, we take $N = 4$ to obtain the approximate responses with a minimal mean square residual error [Wang and Guo (2000)]. In our previous researches [Zhang, Xu and Fang (2007)], the effectiveness of this method with finite number $N = 4$ has been verified.

Then substituting Eq. 4 into Eq. 3, the Eq. 3 is transformed as:

$$\sum_{i=0}^4 \ddot{x}_i(t) H_i(\xi) + (\bar{c} + \sigma \xi) \sum_{i=0}^4 \dot{x}_i(t) H_i(\xi) + (1 + a(\sum_{i=0}^4 x_i(t) H_i(\xi))^2) \cdot \sum_{i=0}^4 x_i(t) H_i(\xi) = F \cos \omega t. \quad (5)$$

Thereafter, by applying properties and recurrent formulas of Chebyshev polynomi-

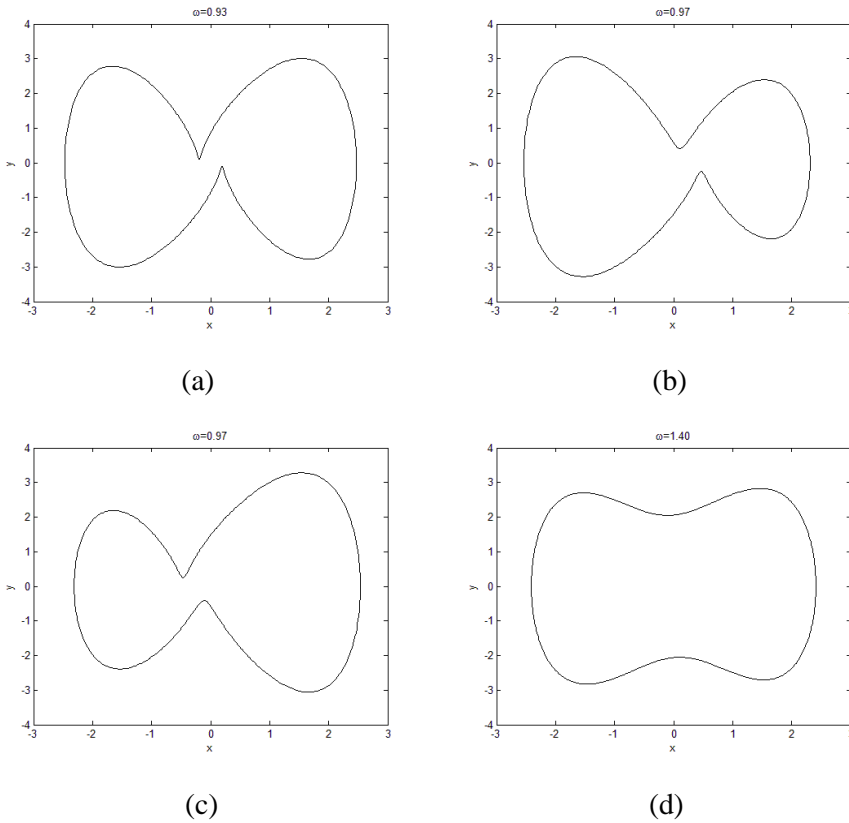


Figure 3: The periodic phase trajectories of Eq.2: (a) $\omega = 0.93$; (b) and (c) are with two different ICs for $\omega = 0.97$; (d) $\omega = 1.40$.

als to Eq.5, the EDS is obtained as

$$\begin{cases} \ddot{x}_0 + \bar{c}\dot{x}_0 + \frac{1}{2}\sigma\dot{x}_1 + x_0 + aX_0 = F \cos \omega t \\ \ddot{x}_1 + \bar{c}\dot{x}_1 + \frac{1}{2}\sigma(\dot{x}_0 + \dot{x}_2) + x_1 + aX_1 = 0 \\ \ddot{x}_2 + \bar{c}\dot{x}_2 + \frac{1}{2}\sigma(\dot{x}_1 + \dot{x}_3) + x_2 + aX_2 = 0 \\ \ddot{x}_3 + \bar{c}\dot{x}_3 + \frac{1}{2}\sigma(\dot{x}_2 + \dot{x}_4) + x_3 + aX_3 = 0 \\ \ddot{x}_4 + \bar{c}\dot{x}_4 + \frac{1}{2}\sigma\dot{x}_3 + x_4 + aX_4 = 0 \end{cases}, \tag{6}$$

which is a deterministic system in form, yet depending on some statistical characteristics of the random parameters .

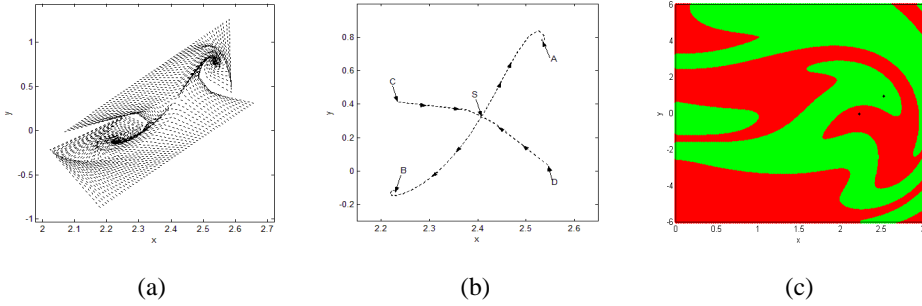


Figure 4: For Eq.2, fixed $\omega = 1.0$: (a) Global pattern of flow lines of Poincaré mapping points around periodic saddle S and periodic node A and B; (b) the refined periodic saddle point and its stable and unstable manifolds, C and D are the initial points; (c) the two coexisting symmetric attractors (black dots) and their basins (green for node A and red for node B).

Let $x_i = x_i$, $\dot{x}_i = y_i$, ($i = 0, \dots, 4$), Eq. 6 can be rewritten as:

$$\begin{cases} \dot{x}_0 = y_0 \\ \dot{y}_0 = -\bar{c}y_0 - \frac{1}{2}\sigma y_1 - x_0 - aX_0 + F \cos \omega t \\ \dot{x}_1 = y_1 \\ \dot{y}_1 = -\bar{c}y_1 - \frac{1}{2}\sigma(y_0 + y_2) - x_1 - aX_1 \\ \dot{x}_2 = y_2 \\ \dot{y}_2 = -\bar{c}y_2 - \frac{1}{2}\sigma(y_1 + y_3) - x_2 - aX_2 \\ \dot{x}_3 = y_3 \\ \dot{y}_3 = -\bar{c}y_3 - \frac{1}{2}\sigma(y_2 + y_4) - x_3 - aX_3 \\ \dot{x}_4 = y_4 \\ \dot{y}_4 = -\bar{c}y_4 - \frac{1}{2}\sigma y_3 - x_4 - aX_4 \end{cases} \quad (7)$$

In order to analyze this ten demission system, the ensemble mean responses (EMR) of Eq. 7 can be obtained as:

$$\begin{aligned} E[x(t, \xi)] &= \sum_{i=0}^4 x_i(t) E[H_i(\xi)] = x_0(t) \\ E[y(t, \xi)] &= \sum_{i=0}^4 y_i(t) E[H_i(\xi)] = y_0(t) \end{aligned}, \quad (8)$$

which are the expectation of responses of EDS. Therefore, based on studying EMR, the dynamical behavior of RP-DS in ensemble mean can be explored.

When $\sigma = 0$ or $\xi = 0$, EMR should be equivalent to the deterministic responses (short for DR) of Duffing system (2). In Fig. 5, taking $\omega = 0.91$ and 0.93 , EMR

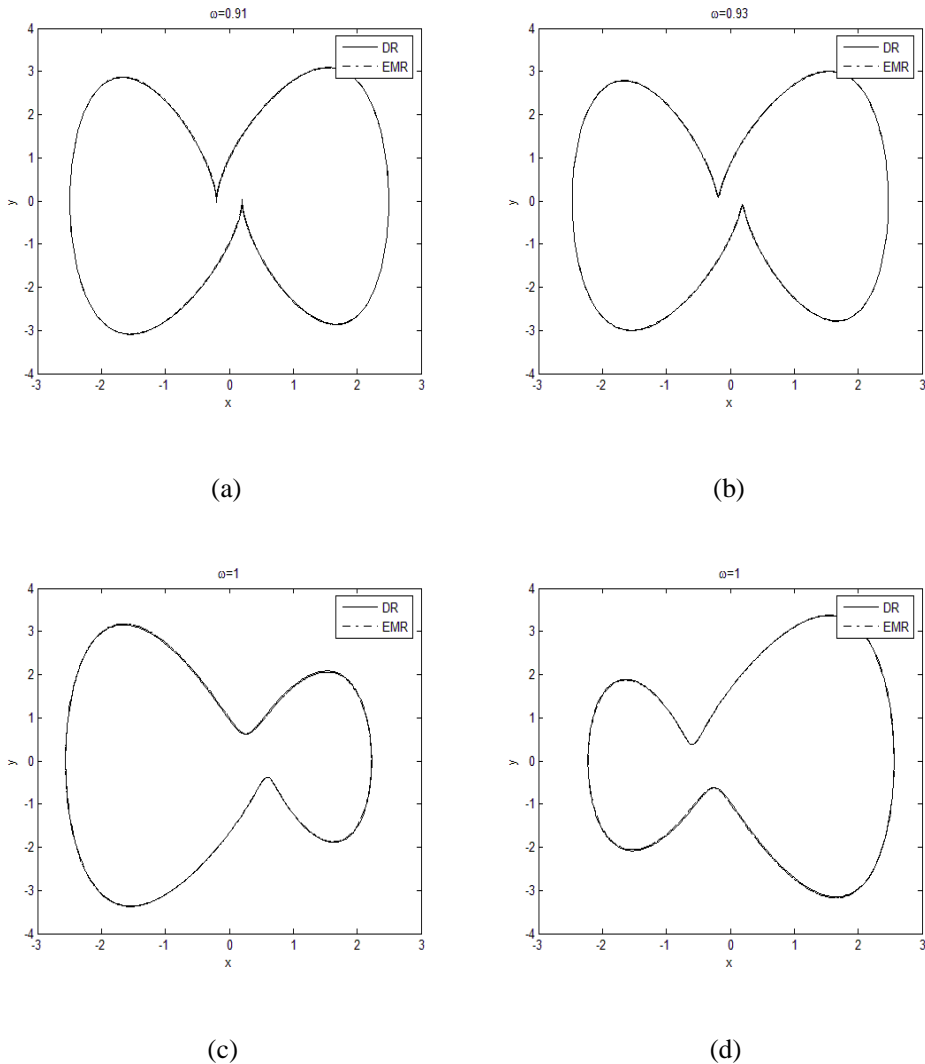


Figure 5: The phase trajectories of DR and EMR with $\sigma = 0$: (a) $\omega = 0.91$; (b) $\omega = 0.93$; (c) $\omega = 1$, CI-1; (d) $\omega = 1$, IC-2.

keeps the single self-symmetric behavior. And for the post SBB at $\omega = 1.0$, the self-symmetric behavior is disappeared and replaced by two coexisting symmetric ones. Since DR and EMR have preferably coherence in Fig. 5 (a)-(d), it is demonstrated that this Chebyshev polynomial approximation method is feasible and effective in this research.

4 Effect of random parameter

The ensemble mean dynamical behaviors of RP-DS are investigated in this section. When $\omega = 0.93$, EMR preserves the same self-symmetric periodic behavior as that in DR-DS before SBB shown in Fig. 6(a). However, with the influence of random factor, the phase trajectories of EMR has been changed a little, and the details are shown in Fig. 6(b) with enlarged scale.

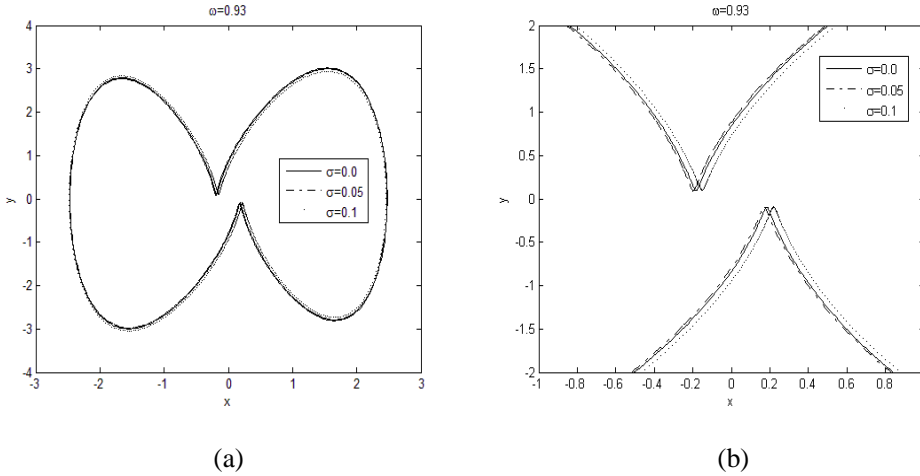


Figure 6: (a) The phase trajectories of EMR at $\omega = 0.93$ for $\sigma = 0.0, \sigma = 0.05$ and $\sigma = 0.1$; (b) The zoom in figure of (a).

After SBB, taking $\omega = 1$ into consideration, the phase trajectories and bifurcation diagrams of EMR are calculated from two different initial conditions shown in Fig. 7. When we do the simulation from IC-1, in Fig. 7(a), the dynamical behavior of EMR is basically the same as that of DR shown in Fig. 5(c), and only a tiny modification is induced by random parameter. In addition, the corresponding bifurcation diagram in Fig. 7(c) also illustrates that EMR is robust when $\sigma \in [0.0, 0.1]$.

Once we choose IC-2 as initial condition, the phase trajectory of EMR, represented by solid line in Fig. 7(b), is symmetry with that calculated from IC-1. But since $\sigma \geq 0.065$, EMR suddenly ‘jumps’ to the other coexisting attractor as shown in Fig. 7(b) by dot line. This phenomenon predicates that RP-DS keeps the same two symmetric attractors as in DP-DS, but due to the effect of random parameter, the two mutual symmetric phase trajectories of EMR are occasionally commutable.

After observing the ‘jumping’ phenomenon by chance, the global analysis is applied to investigate which kind of ICs is unstable under the influence of random

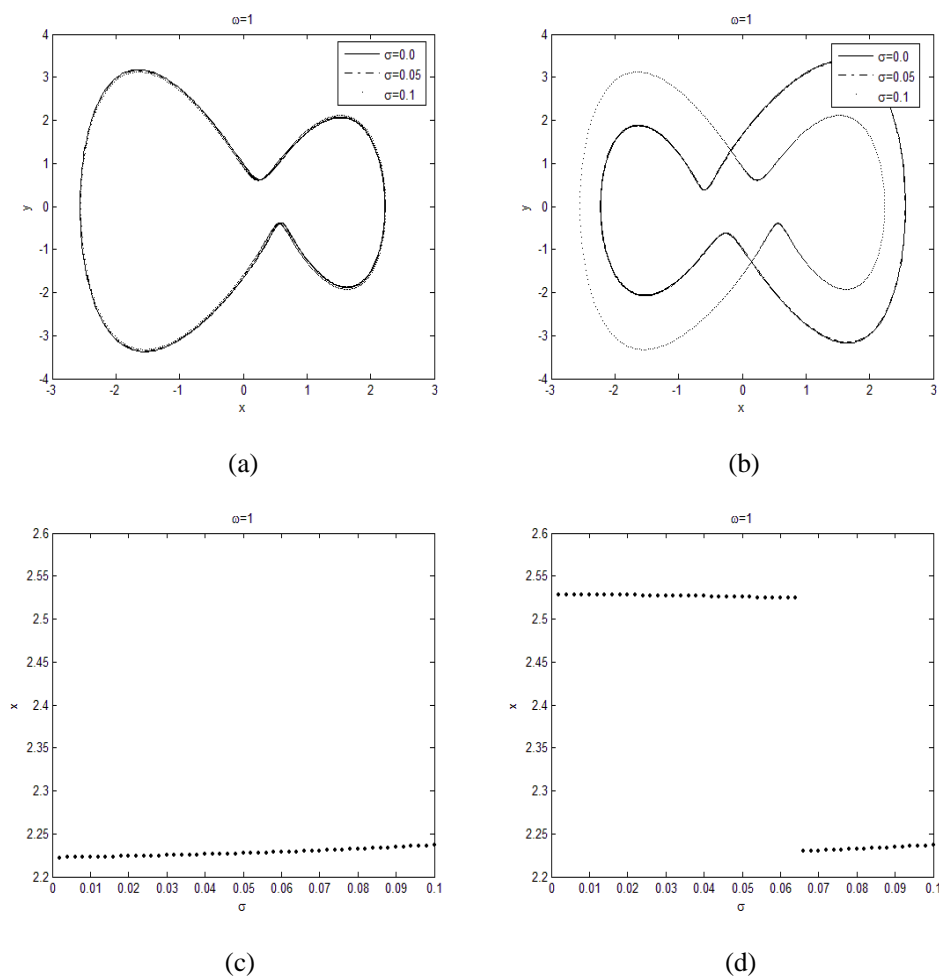


Figure 7: When $\omega = 1$, the phase trajectories of EMR for different intensities: (a) IC-1 and (b) IC-2; The bifurcation diagrams of EMR for $\sigma \in [0.0, 0.1]$: (c) IC-1 and (d) IC-2.

parameter on initial plane. Thus the different features of attractive basins for these two symmetric attractors and the flow lines on Poincaré section are presented in Fig. 8 and Fig. 9.

In Fig. 8, the attractors and their attractive basins for EMR are shown for different value of σ when $\omega = 1$. It is obvious that system preserves the same attractors as that in DP-DS, but the basin boundary is deformed under the influence of random parameter. When $\sigma = 0$, the boundary is still regular and smooth as shown in Fig.

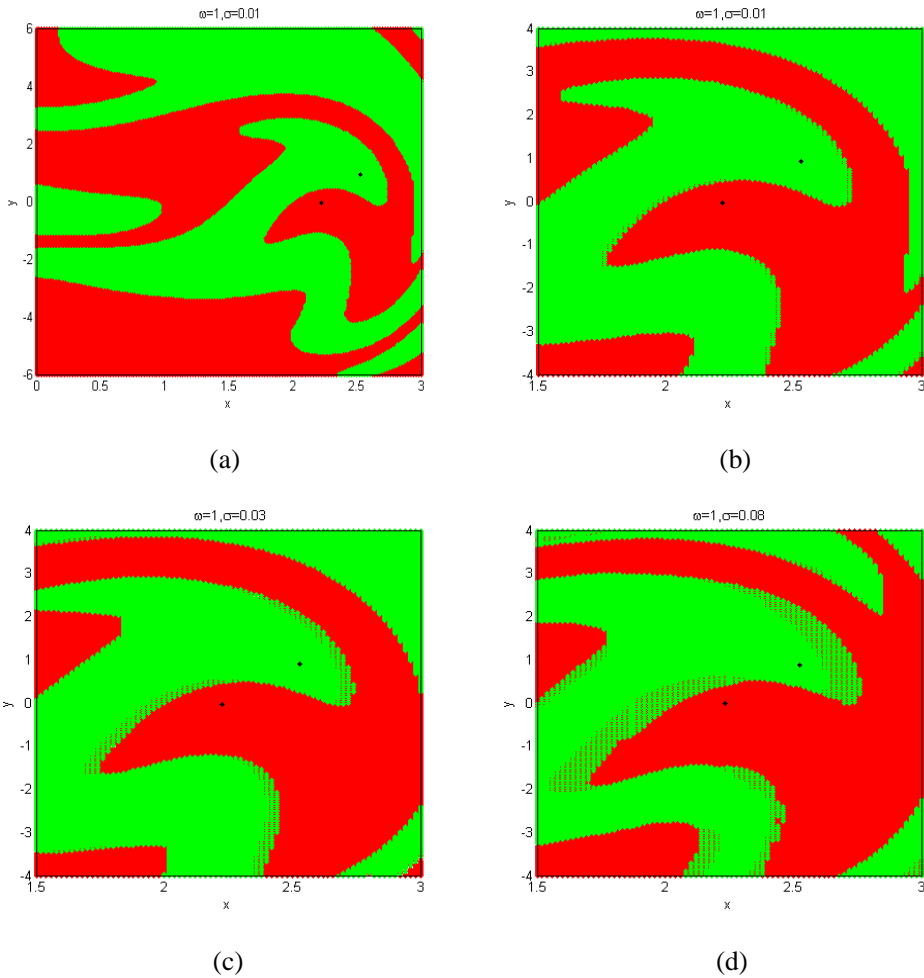
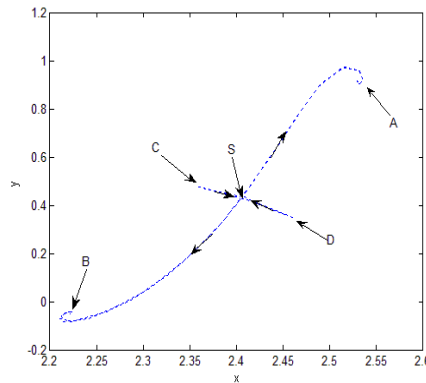
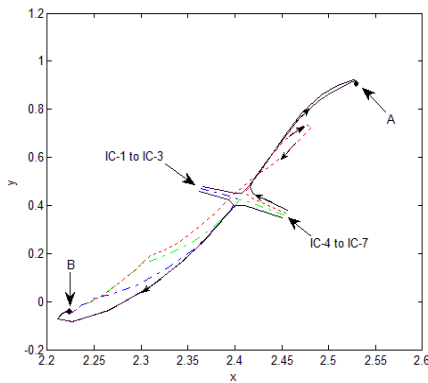


Figure 8: Fixed $\omega = 1$, the two coexisting attractors and their basins of EMR: (a) $\sigma = 0.01$, (b) is the room in figure of (a); (c) $\sigma = 0.03$ and (d) $\sigma = 0.08$, where black dots are attractors, and the red and green regions are attractive basins.

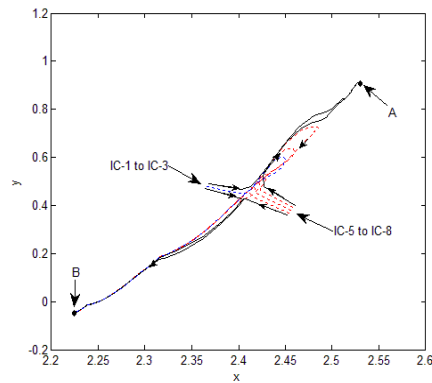
4(c). However with the increasing of σ as in Fig. 8, it is not smooth anymore and become fractal-like. Furthermore, from Fig. 8 (a) to (d), we can see that the bigger the intensity of random parameter is, the wider the basin boundary is. Which mean that the qualitative characteristics of dynamical behavior of RP-DS are not changed with the effect of random parameter, but become sensitive surrounding the basin boundary after SBB in ensemble mean.



(a)



(b)



(c)

Figure 9: When $\omega = 1$, the flow patterns of Poincaré mapping points and attractors of EMR: (a) $\sigma = 0$ with 4 IC points; (b) $\sigma = 0.01$, with 7 ICs and (c) $\sigma = 0.03$, with 8 ICs.

In our previous study of DP-DS, the flow pattern formed by Poincaré mapping points is performed to approximate the position of origin saddle and its invariant stable and unstable manifolds. Herein, the same strategy is applied to study SBB phenomenon in random case. By taking $\sigma = 0$, $\sigma = 0.01$ and $\sigma = 0.03$ for examples, the flow patterns are shown in Fig. 9. It is obvious that RP-DS preserves the same two symmetric attractors as that in DP-DS after SBB, and the ‘jumping’ phenomenon can also be found through the flow patterns close to the invariant manifolds. In Fig. 9, we do numerical simulations from several initial conditions

which are chosen near the invariant manifolds. When $\sigma = 0$, there are no ‘jumping’ events. Observing the red flow line in Fig. 9(b), in deterministic condition, Poincaré points of EMR should go along the unstable manifold and terminal at node A. However, as σ increases from zero to 0.01, the phase trajectory of EMR is changed and eventually attracted by node B. In Fig. 9 (c), it is shown that with bigger intensity $\sigma = 0.03$, the ‘jumping’ phenomenon appears more frequently. That is to say, with increasing of σ , ‘jumping’ region is enlarged around the invariant manifolds, which coincides with the changes in basin boundary.

5 Conclusions

In this paper, dynamical behaviors of SBB with the effect of random parameter are investigated by applying global analysis via invariant stable and unstable manifolds of the original saddle and basins boundary of attractors. In order to analysis SBB phenomena in RP-DS effectively, the Chebyshev orthogonal polynomial approximation method is applied to reduce RP-DS to an EDS to study its dynamical behavior in ensemble average mean. For comparison study, the SBB phenomena in DP-DS are summarized at first. Numerical simulations on both DP-DS and EDS show that SBB may happen in similar apparent forms. However, with the influence of random parameter, the two coexisting symmetric attractors are occasionally commutable, and the corresponding boundary of attractive basins becomes fractal-like, while that in DP-DS case is smooth. In addition, the fractal-like boundary will be enlarged with the increasing of random parameter intensity.

Acknowledgement: This research is supported by the National Natural Science Foundation of China (No. 11302169, 11302171), and the Fundamental Research Funds for the Central Universities (No.3102014JCQ01079, No.3102014JCQ01080).

References

- Bishop, S. R.; Soroniou, A.; Shi, P.** (2005): Symmetry-breaking in the response of the parametrically excited pendulum model. *Chaos, Solitons and Fractals.*, vol. 25, pp. 257-264.
- Chen, Y. H.; Xu, J. X.; Fang, T.** (2001): Observing symmetry-breaking and chaos in the normal form network. *Nonlinear Dyn.*, vol. 24, pp. 231-243.
- Dai, H. H.; Yue, X. K.; Xie, D.; Atluri, S. N.** (2014): Chaos and chaotic transients in an aeroelastic system. *J. Sound Vib.*, vol. 333, pp. 7267-7285.
- Fang, T; Dowell, E. H.** (1987): Numerical simulations of periodic and chaotic responses in a stable Duffing system. *Int. J. Nonlinear Mech.*, vol. 22, pp. 401-425.

Fang, T.; Leng, X. L.; Song, C. Q. (2003): Chebyshev polynomial approximation for dynamic response problems of random system. *J. Sound. Vib.*, vol. 266, pp. 198-206.

Fang, T.; Zhang, Y. (2008): Insight into phenomena of symmetry breaking bifurcation. *Chin. Phys. Lett.*, vol. 25, pp. 2809-2811.

Jensen, H.; Iwan, W. D. (1992): Response of systems with uncertain parameters to stochastic excitation. *J. Eng. Mech.*, vol. 118, pp. 1012-1025.

Ma, S. J.; Shen, Q.; Hou, J. (2013): Modified projective synchronization of stochastic fractional order chaotic systems with uncertain parameters. *Nonlinear Dyn.*, vol. 73, pp. 93-100.

Mei, F. X. (1992): Response of nonholonomic systems with random initial conditions. *Transactions of Beijing Institute of Technology*, vol. 12, no.1, pp. 21-25.

Ott, E. (2002): *Chaos in dynamical systems (2nd edition)*, Cambridge University Press.

Parker, T. S.; Chua, L. O. (1989): *Practical numerical algorithms for chaotic systems*. New York: Springer-Verlag.

Sunner, T.; Sauermann, H. (1993): Bifurcation scenario of a three-dimensional van der Pol oscillator. *Int. J. Bif. and Chaos*, vol. 3, pp. 399-404.

Spanos, P. D.; Ghanem, R. G. (1989): Stochastic finite expansion for random media. *J. Eng. Mech. Div ASCE.*, vol. 115, pp. 1035-1053.

Thompson, J. M. T.; Stewart, H. B. (1986): *Nonlinear Dynamics and Chaos*. Chichester: John Wiley and Sons.

Wang, Z. X.; Guo, D. R. (2000): *Introduction to special functions*. Peking University, Beijing.

Xu, Y.; Ma, S. J.; Zhang, H. Q. (2011): Hopf bifurcation control for stochastic dynamical system with nonlinear random feedback method. *Nonlinear Dyn.*, vol. 65, pp. 77-84.

Xu, Y.; Gu, R. C.; Zhang, H. Q.; Xu, W.; Duan, J. Q. (2011): Stochastic bifurcations in a bistable Duffing-Van der Pol oscillator with colored noise. *Phys. Rev. E*, vol, 83, pp. 056215.

Xu, Y.; Feng, J.; Li, J. J.; Zhang, H. Q. (2013): Stochastic bifurcation for a tumor-immune system with symmetric Levy noise. *Physica A.*, vol. 392, pp. 4739-4748.

Xu, Y.; Feng, J.; Li, J. J.; Zhang, H. Q. (2013): Levy noise induced switch in the gene transcriptional regulatory system. *Chaos*, vol. 23, pp. 013110.

Xu, Y.; Li, Y. G.; Liu, D.; Jia, W. T.; Huang, H. (2013): Responses of Duffing

oscillator with fractional damping and random phase. *Nonlinear Dyn.*, vol. 74, pp. 745-753.

Xu, Y.; Li, Y. G.; Liu, D. (2014): Response of fractional oscillators with viscoelastic term under random excitation. *ASME J. Comput. Nonlinear Dyn.*, vol. 9, pp. 031015.

Xu, Y.; Feng, J.; Xu, W.; Gu, R. C. (2015): Probability Density Transitions in the FitzHugh-Nagumo Model with Lévy Noise. *CMES-Comp. Model. Eng. Sci.*, accepted.

Yue, X. L.; Xu, W.; Zhang, Y. (2012): Global bifurcation analysis of Rayleigh-Duffing oscillator through the composite cell coordinate system method. *Nonlinear Dyn.*, vol. 69, pp. 437-457.

Yue, X. K.; Xu, Y.; Yuan J. P. (2013): Approximate stationary solution for Beam-Beam interaction models with parametric Poisson white noise. *CMES-Comp. Model. Eng. Sci.*, vol. 93, no. 4, pp. 277-291.

Zhang, Y.; Xu, W.; Fang, T. (2007): Stochastic Hopf bifurcation and chaos of stochastic Bonhoeffer-van der Pol system via Chebyshev polynomial approximation. *Appl. Math. Comput.*, vol. 190, pp. 1225-1236.

Zhang, Y.; Xu, W.; Fang, T. (2007): Stochastic period-doubling bifurcation analysis of stochastic Bonhoeffer-van der Pol system. *Chin. Phys.*, vol. 16, pp. 1923-1933.

Zhang, Y.; Lei, Y. M.; Fang T. (2009): Symmetry breaking crisis of chaotic attractors. *Acta. Phys. Sin.*, vol. 58, pp. 3799-3807.

Zhang, L.; Guo, S. (2013): Hopf bifurcation in delayed van der Pol oscillators. *Nonlinear Dyn.*, vol. 71, pp. 555-568.

